Jpn. J. Appl. Phys. Vol. 39 (2000) pp. 3907–3914
Part 1, No. 7A, July 2000

Magnetoluminescence Study of Annealing Effects on the Electronic Structure of Self-organized InGaAs/GaAs Quantum Dots

A. R. GOÑI, H. BORN, R. HEITZ, A. HOFFMANN, C. THOMSEN, F. HEINRICHSDORFF and D. BIMBERG
Institut für Festkörperphysik, Technische Universität Berlin, Hardenbergstr. 36, 10623 Berlin, Germany

(Received January 11, 2000; accepted for publication April 4, 2000)

We have studied the effects of annealing a self-organized InGaAs/GaAs quantum dot sample between 580 and 700°C by magnetoluminescence measurements at 2 K and fields up to 15 T. High-excitation power density luminescence spectra reveal up to three features in addition to the ground-state emission arising from radiative recombination processes between excited states of the quantum dots. With increasing annealing temperature all emission lines shift to higher energies while varying their splittings indicating a systematic increase in volume and Ga content of the dots. From the diamagnetic shift and the Zeeman splitting of the ground-state emission we obtain an increase of the spatial extent of the exciton wave function but a decrease of the effective g-factor upon annealing. The magnetic field splittings of excited-state transitions exhibit a strong dependence on annealing and are well accounted for within a simple oscillator model with total angular momentum mainly determined by the dot envelope functions.

KEYWORDS: quantum dots, magnetoluminescence, 0D electronic states

1. Introduction

Semiconductor technology has experienced a recent breakthrough exploiting the self-organized growth of zero-dimensional (0D) structures, so-called quantum dots (QD), which display highly homogeneous size distributions and large quantum efficiencies for light emission. The InGaAs/GaAs system, for instance, has been increasingly used as active medium in semiconductor lasers because of their peculiar optical and electronic properties.[1)] Carrier confinement to lengths of the order of the de-Broglie wavelength leads to the formation of 0D-like density of states with sharp peaks at discrete energy levels and to an enhanced excitonic binding, both contributing to improve the performance of quantum dot devices.[2)] Although electronic states in such artificially made atoms exhibit shell-like arrangements having angular momentum as a good quantum number,[3–5)] a detailed description of their energy spectrum ought to take into account the effects of dot shape, built-in strain, and piezoelectric fields.[6–9)]

As a result of the simultaneous strong confinement of electrons and holes, exciton formation is readily achieved in quantum dots with binding energies typically reaching values of several tens of meV.[8–11)] Since the exciton ground-state properties are determined by the interplay between Coulomb interaction and confining potential, magnetooptical studies of the band-edge emission[12–15)] and absorption[16,17)] yielded valuable information about band structure and crystal-field symmetry, i.e., dot shape. For the $In_xGa_{1-x}As/GaAs$ dot system with $x > 0.5$ the large built-in strain splits the top of the valence band such that the ground-state exciton has heavy-hole character. At zero magnetic field and neglecting the electron-hole exchange interaction which is important only for nanometer size crystals,[11)] the heavy-hole exciton is four-fold degenerate, its states being characterized by the total angular momentum components $\pm 1, \pm 2$ along the z direction. They correspond to the so-called *bright* and *dark* excitons, respectively.[12)] Nevertheless, the dark components can become optically active due to the admixture with the bright ones caused by shape asymmetries. In the presence of a large magnetic field and provided that the four emission lines associated with the heavy-hole exciton recombination can be resolved in optical spectra, both the electron and hole g-factors can be determined for the dot structure under consideration.[15)] Magnetic field effects, however, are much more pronounced for excited states of QD's resulting in large shifts and splittings of optical transitions, which serve as a stringent test of model calculations in 0D.[11,18–22)]

In aiming to unreveal the electronic structure of QD's, the application of high hydrostatic pressure has proved to be very useful.[23,24)] For example, the origin of the high-energy luminescence lines appearing in dot spectra has been clarified by using the pressure-induced Γ–X crossover effect in the conduction band as due to transitions from *different* excited electron states.[25)] Another way of modifying dot parameters for a single structure consists in thermally annealing a sample at different temperatures while doing the optical characterization.[26–31)] In spite of the strong intermixing of group-III elements, which occurs for the InGaAs/GaAs system at elevated temperatures, a significant narrowing and blueshift of the dot emission is usually attained after thermal annealing.[27–29)] Since the wetting layer luminescence, on the contrary, is only slightly affected by the annealing process, these results indicate a reduction of carrier confinement which can have a negative effect on the performance of devices working at room temperature. Thus, depending on the particular application one has to find a compromise between sharpness of the dot-size distribution and the strength of confinement in deciding the best set of growth parameters like the temperature or the composition of dot and barrier material.

In this work we have combined for the first time the power of magnetoluminescence experiments for electronic-structure studies with the possibility of varying quantum-dot parameters in a systematic way by thermal annealing. Here we present photoluminescence (PL) measurements for a series of five thermally annealed self-organized InGaAs/GaAs QD samples in magnetic fields up to 15 T. The use of a high-power density for the excitation of the luminescence allows us to observed up to three emission lines arising from optical transitions between excited states of the dots. From changes in magnetooptical properties like the diamagnetic shift of the ground-state emission, the energy separation between PL peaks, and their magnetic field splittings we infer an increase in Ga content and size of the dots with increasing annealing temperature. The observed dependence on magnetic field of

the lower energy emission lines are well reproduced for all samples using a Luttinger-Kohn model, in which due to the axial symmetry of the confining potential the envelope wave functions are classified by the z components of the angular momentum $\boldsymbol{L}$ calculated within the effective-mass approximation. As an exeption, we observe an unexpected magnetic-field behavior of peaks associated with excited-state QD transitions only in σ^+ circular polarization, which is tentatively ascribed to coupling between heavy and light-hole levels. The discrepancy in the magnetic splittings of PL lines for σ^+ and σ^- polarization disappears rapidly but gradually with annealing. By examining the ratio of the effective exciton diameter for the ground and first excited state, as obtained from the corresponding diamagnetic shifts of the transition energies, we conclude that the simple 2D harmonic oscillator model for QD excitons in a magnetic field is strictly applicable only in the case of the sample annealed at 700°C. Furthermore, we have determined an effective g-factor for the ground-state exciton of the five samples of the annealing series, which compares roughly within a factor of two with the predictions of $\mathbf{k}\cdot\mathbf{p}$ theory.

2. Experimental Details

The as-grown sample consists of a single layer of InGaAs dots embedded in GaAs grown by low-pressure metalorganic chemical vapor deposition (MOCVD) at a temperature of 485°C in the Stranski-Krastanow mode, as described elsewhere.[28] The nominal In concentration of 42% of the InGaAs layer is expected to be substantially higher in the QD's due to In segregation and migration effects. For the as-grown sample the dots have an average base size of 14–19 nm and a height of 6–8 nm, as deduced from transmission electron micrographs (TEM).[28] Individual pieces of the same sample were reinserted into the MOCVD reactor and annealed for 30 min at temperatures between 580°C and 700°C under AsH_3 atmosphere.

Magnetoluminescence measurements up to 15 T were done at 2 K in Faraday configuration with circularly polarized light by inserting the sample in the cold bore of a superconducting split-coil magnet. PL spectra were excited with $\sim$5 kW/cm^2 incident power density from an Ar^+ ion laser (514 nm line). The light emitted from the growth direction was analyzed by a 0.75 m double-grating spectrometer equipped with a LN_2-cooled Ge detector. The luminescence spectra were corrected for the spectral dependences of the various optical components by calibrating the wavelength response of the setup using a black-body emitter.

3. Results and Discussion

At high excitation power densities and zero magnetic field up to three emission lines are apparent from the low-temperature PL spectra at higher energies than that of the ground-state exciton recombination,[28,32] which are attributed to optical transitions between excited confined states of the dots. Figure 1 shows the energy position at $B = 0$ of the PL peaks (labelled as E_i, $i = 0, 1, 2, 3$) in the spectral region of the dot emission for the complete series of annealed samples (the abscissa for the as-grown sample corresponds to the growth temperature of 485°C). With increasing annealing temperature we observe a significant blueshift of the ground-state emission by about 150 meV, whereas the energy separation between excited states is reduced by a factor of two. A striking result concerns the nearly constant energy difference between PL peaks, as displayed by the data points of Fig. 1 for all five samples. This allows us to estimate the bandgap energy E_g by using a simple harmonic oscillator model (see Table I). The gap shifts to higher energies by almost the same amount as E_0. In contrast, the wetting-layer luminescence peaks at an energy between 1.35 to 1.37 eV, hence, it is almost independent of annealing.[28] The average PL linewidth decreases also strongly with annealing being for the sample annealed at 700°C half of the value as for the as-grown one (see Fig. 2). It has been shown that these experimental findings agree qualitatively with a simple model which assumes spherical QD's and Fickian interdiffusion of dot and barrier material.[28]

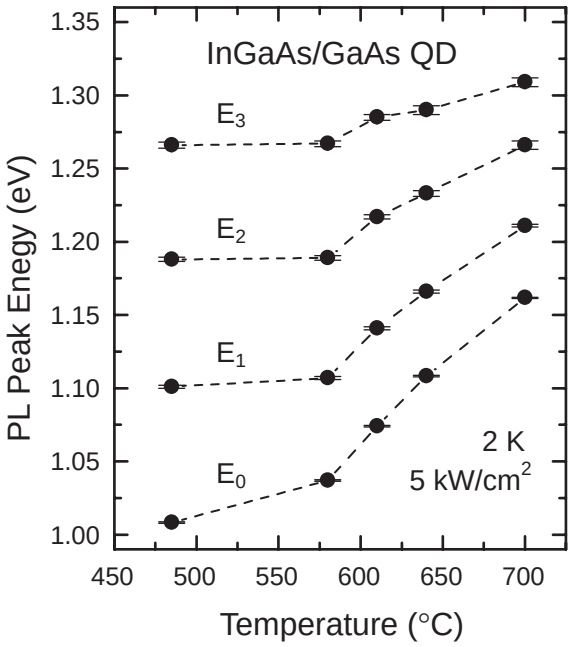

Fig. 1. Energy position of peak maxima observed in the PL spectra of the quantum dots for the annealed series (the growth temperature was taken for the as-grown sample) for high excitation powers at zero magnetic field and at 2 K.

The blueshift of the transition energies with annealing clearly speaks for an additional incorporation of Ga in the dots. One can pursue a rough estimation of the In concentration in the dots by comparing the average shift of the dot emission with the band gaps of $Ga_xIn_{1-x}As$ alloys[33] after correcting for the simultaneous reduction of the built-in strain due to Ga incorporation. In good approximation, the contribution of strain relaxation to the band gap shift is given by the hydrostatic part of a tetragonal stress produced by the lattice mismatch for a given Ga concentration according to:[34]

$$\Delta E_g^{\text{strain}} = -2a_{cv} \cdot \left(1 - \frac{C_{12}}{C_{11}}\right) \cdot \epsilon_{xx} \approx -a_{cv}\epsilon_{xx}, \qquad (1)$$

where $a_{cv} = 8.5$ eV is the hydrostatic deformation potential of the direct bandgap of GaAs,[35] C_{11}, C_{12} are the elastic constants[33] and ϵ_{xx} is the lattice-mismatch strain. This approximation is justified because, in tetrahedral semiconductors, the blueshift of the direct gap at the Γ point of the Brillouin zone arises essentially from the pressure-induced change of the conduction-band edge,[34] for which states are s-like, i.e., there is no additional splitting due to uniaxial-stress compo-

Table I. Several dot parameters for the samples of the annealing series used in the analysis of the magneto-PL data.[33] E_g is the band gap, x is the Ga concentration, ϵ_{xx} is the biaxial built-in strain, $m_{e,0}$, $m_{e,1}$, m_{hh} and $m_{lh,0}$ are the effective masses calculated within $\mathbf{k}\cdot\mathbf{p}$ of the electron ground and first excited state, the heavy hole and the light-hole ground state, respectively, Δ_0 is the valence-band spin-orbit splitting, γ_1, γ_2 and κ are hole Luttinger parameters, g_e, g_h and g^* are the calculated electron, heavy-hole and effective g factors, respectively (see text for details).

Sample	*as grown*	580°C	610°C	640°C	700°C
E_g (eV)	0.99(3)	1.01(2)	1.04(2)	1.075(15)	1.135(15)
x	0.00(8)	0.10(5)	0.20(5)	0.30(5)	0.45(5)
ϵ_{xx} (%)	−6.7(8)	−6.1(5)	−5.4(5)	−4.8(5)	−3.8(5)
$m_{e,0}$ (a.u.)	0.045	0.046	0.047	0.048	0.051
$m_{e,1}$ (a.u.)	0.048	0.048	0.049	0.050	0.052
m_{hh} (a.u.)	0.35	0.35	0.35	0.35	0.35
$m_{lh,0}$ (a.u.)	0.061	0.062	0.064	0.066	0.069
Δ_0 (eV)	0.380(10)	0.375(10)	0.370(10)	0.365(10)	0.360(10)
γ_1 (a.u.)	9.6	9.4	9.1	8.8	8.3
γ_2 (a.u.)	3.4	3.35	3.25	3.15	3.1
κ (a.u.)	1.76	1.77	1.71	1.66	1.71
g_e	−7.2(7)	−6.8(7)	−6.4(6)	−6.0(6)	−5.2(5)
g_h	−3.3(4)	−3.1(4)	−2.9(3)	−2.8(3)	−2.3(2)
g^*	−1.27(13)	−1.21(12)	−1.19(12)	−1.15(12)	−0.82(8)

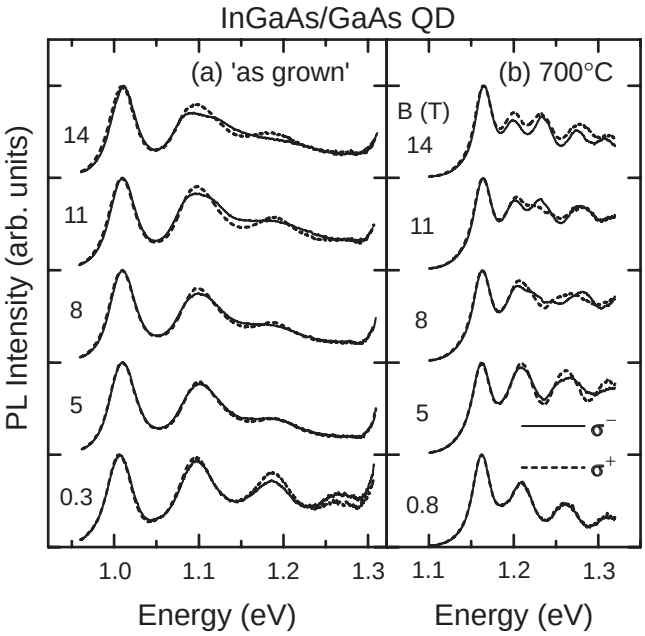

Fig. 2. Photoluminescence spectra of an InGaAs/GaAs quantum dot structure (a) as grown and (b) annealed at 700°C measured using high excitation powers of 5 kW/cm^2 for different magnetic fields and at 2 K. The solid (dashed) lines correspond to σ^- (σ^+) circular polarization.

nents. The results for the Ga content x are listed in Table I. We obtain a 45% increase in Ga concentration for the 700°C sample, as compared with the as-grown one, for which the dots seem to be of pure InAs. This is, in fact, fully supported by atomically-resolved cross-sectional micrographs obtained by scanning-tunneling microscopy (STM) on samples containing threefold stacked QDs grown under exactly the same conditions as ours.[36,37] The STM pictures exhibit several pyramidal shaped dots consisting of stoichiometrically pure InAs (Ga content less than 2%). Such strong reduction of the Ga concentration in dots with nominal 42% In of the InGaAs layers is ascribed to In migration during growth.[28] We like to point out that these concentrations have to be taken as average values for the core region of the dots. In addition, thermal annealing causes an enhancement of the dot size, as indicated by the smaller energy separation between PL peaks at higher annealing temperatures. We show below from magnetooptical experiments that the concomitant volume change consists most likely of a preferential increase of the dot height with respect to base.

Application of a strong magnetic field in the growth direction has an impact on the PL emission of the dots in Faraday configuration. In Fig. 2 we show the magnetic field dependence of the PL spectra for the two limiting cases, i.e., for the *as grown* and the 700°C annealed sample. The emission at E_0 displays for all the samples of the series the characteristic diamagnetic shift of an excitonic ground state and a very small Zeeman splitting of the order of 1 meV. In contrast, the excited state PL lines exhibit large splittings of up to 30 meV at 14 T depending on circular polarization of the emitted light. Interestingly, the magnetic-field behavior of both the σ^+ and σ^- polarizations is very different for each sample pointing to the peculiarities of their electronic structure.

The evolution of the PL emission with magnetic field has been analyzed by performing lineshape fits to the spectra for both polarizations using a series of Gaussian peaks: one for the ground state, two for the first excited state and three for each of both remaining high-energy peaks observed at $B = 0$. In order to reproduce the continuous splitting of lines with increasing field, we kept all linewidths constant at their initial values for zero field. We remark here that excited dot levels were considered manyfold degenerate at zero magnetic field in spite of the fact that calculations within 8-band $\mathbf{k}\cdot\mathbf{p}$ theory[8] and an atomistic pseudopotential approach[9] predict the lift of degeneracy due to piezoelectric fields. Nevertheless, for the dot sizes in our samples the splittings are at most about 10 to 15 meV large, which we are unable to resolve with PL linewidths ranging from 30 to 60 meV. Therefore, for the sake of simplicity we will disregard piezoelectric splittings in the discussion hereafter. In Figs. 3(a) to 3(e), the energy position of the peak maxima is plotted as a function of magnetic field (symbols) for the five samples studied here. The data exhibit following systematics: In each polarization, the E_0 peak does not split but shift diamagnetically, E_1 splits into two lines, E_2 and E_3 into at least three peaks each one, as far as we are able to resolve with the Gaussian fitting procedure. The magnitude of the splitting increases for higher excited states. The solid curves represent theoretical results for the magnetic field dependence of the excitonic dot levels calculated as discussed below. For the highest excited states there are more predicted transitions splitting in magnetic field, as are actually resolved.

Our InGaAs/GaAs QD samples are characterized by confinement energies for electrons and holes ranging between 30 and 60 meV as well as large binding energies for the ground-state exciton in excess of 20 meV.[8,9] This enables the treatment of the effects of an external magnetic field B in a perturbative manner. In the framework of the effective mass approximation, the energy shift of the emission lines with B can be written as[38]

$$\Delta E_i = \Delta E_{\text{Diamag.}} + \Delta E_{\text{Zeeman}}. \qquad (2)$$

The first term is quadratic in the field and corresponds to the

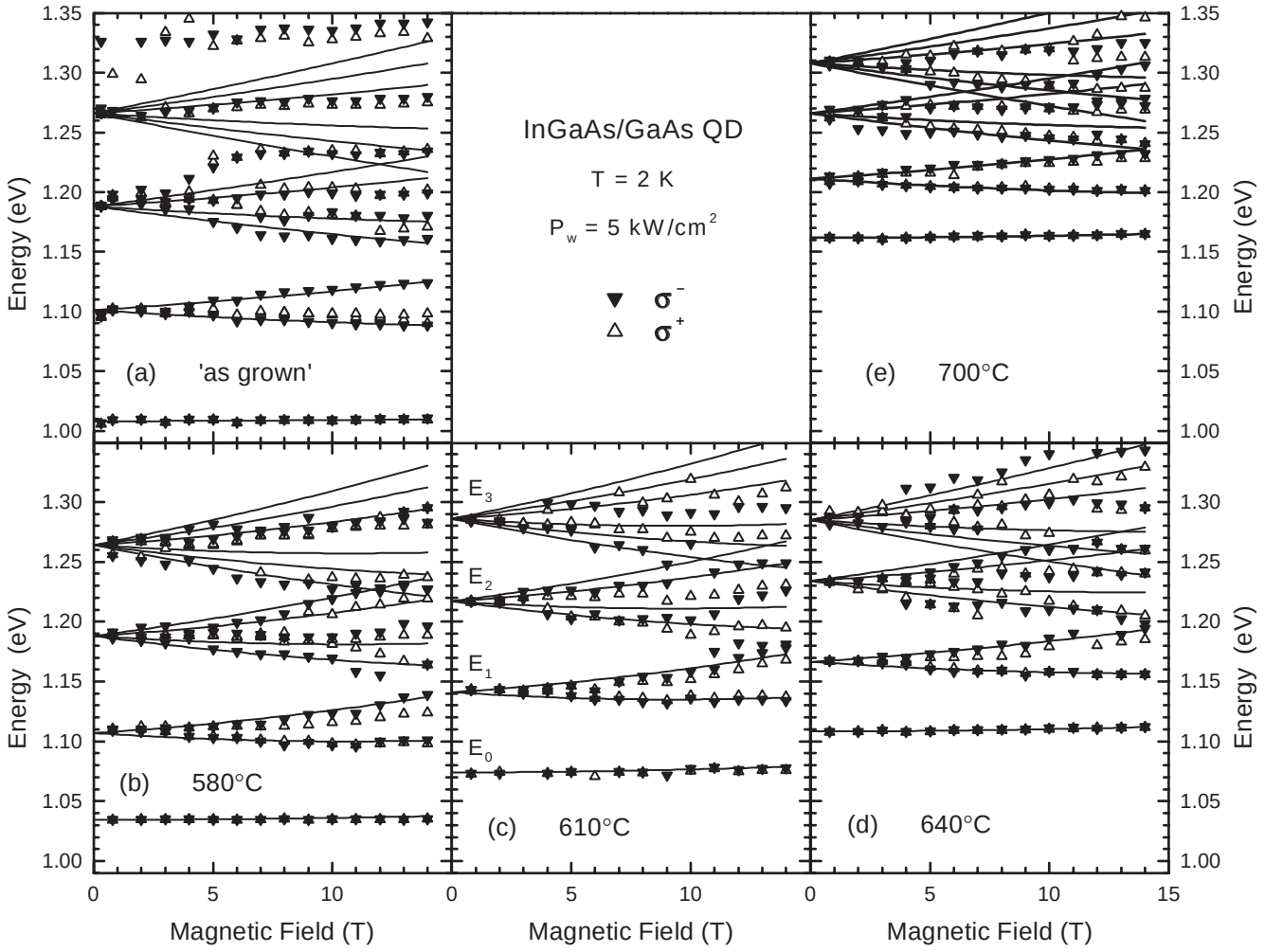

Fig. 3. Magnetic-field dependence of the peak energies of PL lines for (a) the as-grown sample and the samples annealed at (b) 580°C, (c) 610°C, (d) 640°C and (e) 700°C. Solid (open) symbols correspond to σ^- (σ^+) circular polarization. Solid lines represent the results of calculations using eqs. (2), (3) and (5) with the parameters of Table I.

diamagnetic contribution to the electron energy coming from the quantization of its orbital motion. For an exciton it is approximately given by

$$\Delta E_{\text{Diamag.}} = \frac{e^2}{12\mu}\langle r^2\rangle B^2, \tag{3}$$

where $\langle r^2\rangle$ is the square of the average radius of a sphere containing the exciton wave function and $1/\mu = 1/m_e + 1/m_h$ is the inverse of the reduced mass with m_e and m_h the electron and hole effective masses, respectively. The second term in eq. (2) is linear in B and represents the Zeeman level splitting due to the alignment of the net magnetic moments of the electrons and holes in the magnetic field. Its explicit form is different for the ground state E_0 as compared to the excited states because of the different origin of the total angular momenta giving rise to the magnetic properties of the particular level. For the ground state the Zeeman term is purely of *atomic* origin (the atomic part of the Bloch wave functions) and represents the splitting between the σ^+ and σ^- circularly polarized emission lines

$$\Delta E^{\text{GS}}_{\text{Zeeman}} = \pm g^* \mu_B B, \quad \text{for } \sigma^\pm \text{ polarization.} \tag{4}$$

Its magnitude is thus determined by an effective Landé factor g^* for the exciton times the Bohr magneton μ_B. The quantity g^* contains both the contributions from the electron and hole Zeeman splitting. For the excited states the main contribution to the exciton magnetic moment arises from the orbital motion in the confining potential described by the envelope wave functions of the discrete dot levels.[19] Assuming that self-organized quantum dots possess axial symmetry along the growth direction, the envelope functions can be decompose into eigenstates of the angular momentum $\boldsymbol{L}$ with components $L_z = M_L\hbar$. The Zeeman term of eq. (2) takes the form

$$\Delta E^{ES}_{\text{Zeeman}} = \frac{\mu_B M_L}{\mu} \cdot B. \tag{5}$$

Both cases will be considered in detail below.

We turn now to the discussion of the diamagnetic shifts for the ground and the first excited-state transitions. Figure 4(a) shows the diamagnetic-shift values for the ground state, as obtained from the slope of a plot of $(E_0^+ + E_0^-)/2$ versus B^2, where the $+, -$ index stands for σ^+, σ^- polarization. Using eq. (3) it is possible to obtain the spatial extension of the exciton wave function given by the mean diameter $2\sqrt{\langle r^2\rangle}$ provided the exciton reduced mass μ is known. For this purpose we have calculated the electron effective mass within **k·p** theory,[34,39] whereas the effective heavy-hole mass was taken as constant[33] (see Table I). Here we like to stress the point that the **k·p** effective masses are independent of the par-

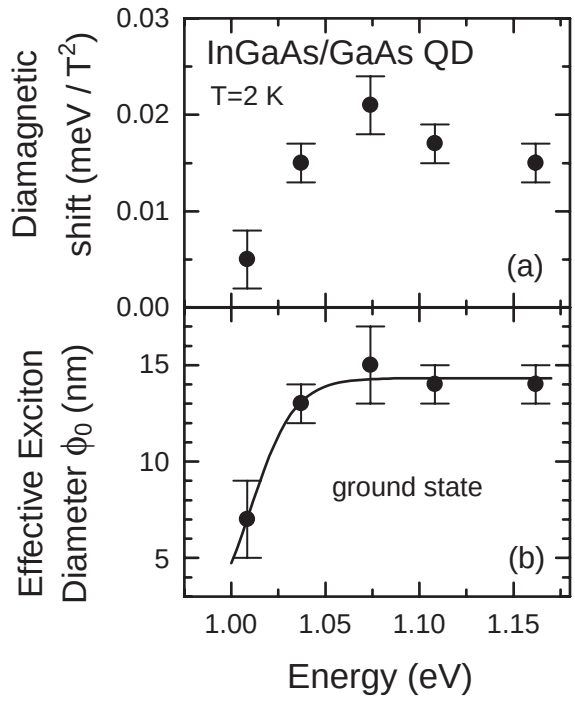

Fig. 4. (a) Diamagnetic shift and (b) average exciton diameter ϕ_0 of the dots exciton ground state as a function of the emission energy E_0 for the annealing series. Line is a guide to the eye.

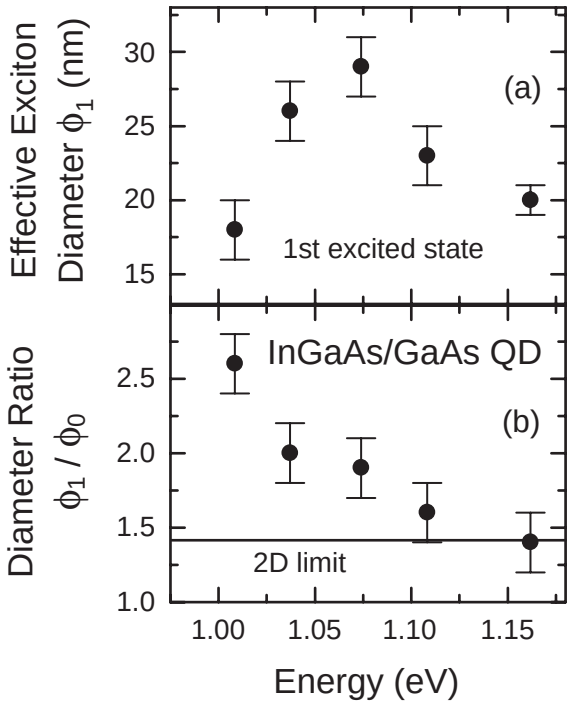

Fig. 5. (a) Effective exciton diameter ϕ_1 of the first excited state of the dots and (b) diameter ratio between ground state and 1^{st} excited one for the annealing series. The line indicates the expected ratio for a 2D harmonic oscillator.

ticular model used for the estimation of band gap, strain or alloy composition of the dots. They are mainly determined by the measured PL transition energies. Thus, further analysis of our data using the masses listed in Table I is not much influenced by the assumptions made before. The results for the effective exciton diameter ϕ_0 of the ground state are plotted in Fig. 4(b) as a function of E_0 for the five samples of the series. The solid curve is just a guide to the eye. In agreement with the size increase of the dots derived from PL measurements at zero field, we observe an initial increase by roughly a factor two of the effective exciton diameter with annealing. For the *as grown* sample the exciton diameter appears to be determined by the dot height, whereas for the annealed samples the exciton size reaches a constant value which is in the range of the dot base size for the as-grown sample. We note that the value at which ϕ_0 saturates also corresponds to twice the Bohr radius of a 2D exciton with 30 meV binding energy. For comparison, the binding energies calculated for pyramidal InAs dots embedded in GaAs are of the same order.[8,9]

The effective exciton diameter ϕ_1 of the first excited state can be derived from the diamagnetic shift of the E_1 transition by taking the average $(E_1^-(+1) + E_1^-(-1))/2$ between splitted branches with ± 1 projection of angular momentum but only for the σ^- polarization. The splitting of lines for light with σ^+ polarization is further influenced by an additional interlevel coupling, as discussed below. Figure 5(a) shows the results for ϕ_1 versus the ground-state energy. In contrast to the behavior displayed by ϕ_0, the exciton diameter of the 1st excited state reaches a maximum for the sample annealed at 610°C. Nevertheless, the ratio between both exciton diameters decreases monotonically with annealing, as indicated by the data points in Fig. 5(b). It is interesting to note that the solid line corresponds to the expected ratio for a 2D harmonic oscillator. Although this is a model commonly used to describe the behavior of confined excitons in a magnetic field, we are led to conclude that for our dot structures this is a good approximation only for the sample annealed at the highest temperature of 700°C.

Let us consider the magnetic-field splitting between both circular polarization components of the ground state emission (1.5–0.7 meV at 14 T). The physical situation for the optical transitions is depicted schematically in Fig. 6. The envelope functions of the ground-state electron and hole levels are *s*-like, i.e. their net angular momentum vanishes ($M_L \equiv 0$). Each state, however, exhibits a small Zeeman splitting associated with the lifting of degeneracy due to the *atomic* total angular momentum $\boldsymbol{j}$ with z components M_j. In the case of the holes, we consider the ground-state to be of heavy-hole character, assumption which is supported by several band-

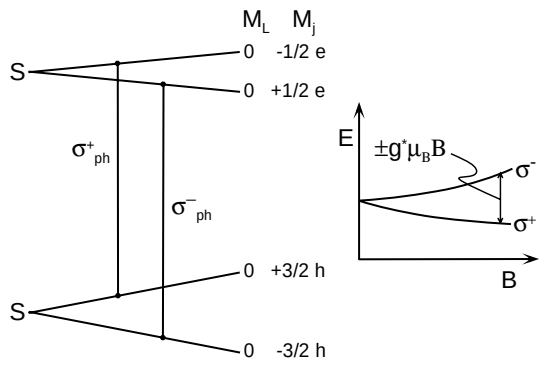

Fig. 6. Level scheme indicating allowed optical transitions between electron and hole ground states of the quantum dots. States are labelled according to their z component M_L of the envelope angular momentum and M_j of the atomic one. The inset schematically represents the energy splitting of the corresponding emission with $\sigma^{\pm}$ polarization in a magnetic field.

structure calculations.[8,9,11] As indicated in Fig. 6, the selection rules for allowed optical transitions are $\Delta M_L = 0$, $\Delta M_j = \pm 1$, which results in emission of light with either left or right-handed circular polarization (note that letter e and h denotes electron and hole quantum numbers, respectively). In our experiments, the σ^+ component is lower in energy and its Zeeman splitting to the σ^- polarization grows linearly with magnetic field. The corresponding coefficients are shown in Fig. 7(a) for all five samples. Thus, the Zeeman splitting decreases with annealing by more than a factor of two.

Figure 7(b) shows the effective g^* factors of the annealing series as obtained from the Zeeman splitting of the E_0 transition using eq. (4). Similar splittings have been recently reported for the same material system from single-dot spectroscopy.[13,15] With annealing we observe a decrease in magnitude of the g factor. Further insight into the dependence of g^* on dot size and composition can be gained by analyzing the separate contributions from electron and hole. For heavy-hole excitons the g factor is given by[11,40,41]

$$g^* = \frac{|g_e| - 3|g_h|}{2},$$

where g_e and g_h are the electron and hole g factors, respectively. The electron g factor is negative and can be calculated within $\mathbf{k}\cdot\mathbf{p}$ theory as[42]

$$g_e \approx 2\left\{1 + \frac{m_e - 1}{m_e}\left(\frac{\Delta_0}{E_g + 2\Delta_0}\right)\right\}, \qquad (6)$$

with Δ_0 the spin-orbit splitting of the valence band at the Γ point of the Brillouin zone. For the hole g factor we have simply taken the expression holding for quantum wells, which is given within effective-mass theory in terms of Luttinger parameters as[41]

$$g_h = \frac{2}{3}\cdot\left(3\kappa - \gamma_1 - \gamma_2 + \frac{1}{m_{hh}}\right), \qquad (7)$$

with $\gamma_1 = (m_{hh}^{-1} + m_{lh}^{-1})/2$, $\gamma_2 = (m_{lh}^{-1} - m_{hh}^{-1})/4$, and $\kappa = -\gamma_1/3 + 5\gamma_2/3 - 2/3$, in atomic units.[43,44] The results for g_e, g_h and g^* are listed in Table I together with the Luttinger parameters. Using these values we obtain the effective g factors represented by the dashed line in Fig. 7(b). Although the calculated absolute values for g^* are off by a factor of two to three as compared to the measured ones, the decrease of g^* with annealing is reproduced. This tendency is in accord with the expected behavior of the electron and hole g factors. The former changes from -15 to -0.44 in bulk InAs and GaAs, respectively, mainly due to the increase of the electron effective mass m_e and the reduction of the Δ_0/E_g ratio between spin-orbit coupling and band gap.[42] The hole g factor is negative too and decreases due to the enhancement of m_{lh} upon Ga incorporation. In perspective, the discrepancy between experimental and theoretical effective g factors demonstrates the need of more accurate calculations of g^* for quantum dots taking into account actual dot shape and level mixing, a task which seems not possible at present.

It is instructive to compare the g factors obtained here with those determined by single-dot spectroscopy,[15] in which case, the extremely narrow linewidths due to suppression of inhomogeneous broadening enable the resolution of the four Zeeman splitted heavy-hole exciton states. This is clear evidence of strong exciton state mixing effects arising from shape asymmetries of the dots leading to the relaxation of selection rules for optical transitions.[11] Interestingly, our g^* values are in very good quantitative agreement with the effective g factor determined for the dark exciton components rather than the bright ones.[15] The dimensionality of the system seems to play a similarly important role as geometry in determining the magnitude of g factor. For instance, in the case of 10 nm wide $In_{0.53}Ga_{0.47}As/InP$ quantum wells, g^* is negative but a factor of two smaller than for our dots,[41] whereas for InAs monolayers in bulklike GaAs it reverses its sign, i.e. the σ^- polarization becomes lower in energy with increasing magnetic field.[45] A change in sign of the heavy-hole g factor is at the origin of this effect. Furthermore, we point out that there is experimental evidence for the effective g factor being dependent on excitation power. This might be a consequence of many-body effects which become important as the quantum dots are filled with excitons at higher excitation levels.[46]

Finally, we consider the effects induced by magnetic field on the excited states [see Figs. 3(a)–3(e)]. As pointed out above, their splittings are too large for being of atomic origin but they rather arise from the Zeeman coupling of the angular momentum associated with the excitonic envelope function in the dots and the external magnetic field.[19] Figure 8 illustrates the situation for the optical transitions between the first excited electron and hole states, which are characterized by having p-type envelope functions. Again, we only consider the heavy component of the holes and disregard possible piezoelectric level splittings at $B = 0$. The $M_L = 0$ levels are intentionally omitted for the excited states because optical transitions betweem them are forbidden for emission from the growth direction. As indicated in the inset to Fig. 8, we expect two pairs of lines with $\sigma^\pm$ polarizations, whose splitting

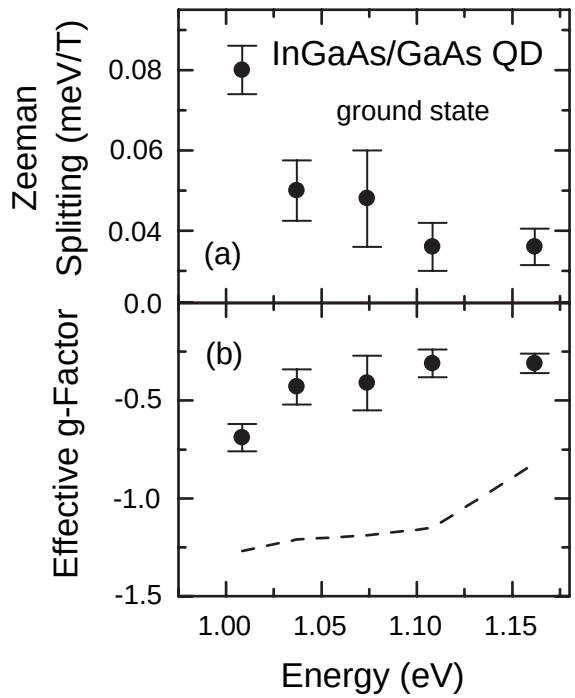

Fig. 7. (a) Zeeman splitting and (b) effective g factor g^* of the ground state for the annealing series. The dashed curve represents the calculated values for g^* using the electron and hole g factors from eqs. (6) and (7), respectively.

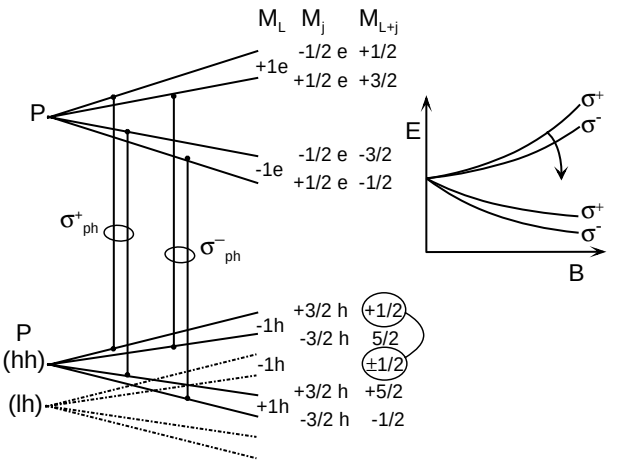

Fig. 8. Level scheme indicating allowed optical transitions between the first excited states of the dots. As illustrated in the inset, coupling between heavy and light-hole states of same symmetry (circled ones) leads to a reduction of the magnetic-field splitting of the emission lines in σ^+ polarization.

is given by eq. (5). The solid curves of Figs. 3(a)–3(e) represent the results for the magnetic-field dependence of observed optical transitions calculated using eqs. (2), (3) and (5) in account of the different angular momentum components M_L of each state. For these calculations the **k**·**p** masses of Table I were used. The agreement between measured and calculated energies is remarkably good for the two lowest transitions at E_0 and E_1, for the latter, however, only for σ^- polarization. Similarly strong Zeeman effects for excited states were previously reported for stress-induced QD's.[19,22] In spite of the fact that for these dots the lateral confining potential is expected to be nearly parabolic, the magnetic field dependence of optical transitions is not as well reproduced by the model calculation as for our self-organized structures.

A striking result of this work concerns the distinct magnetic-field behavior of the E_1 transition in σ^+ polarization for the different samples, which allows us to obtain important information about the electronic structure of the self-organized dots. For the sample annealed at 700°C [see Fig. 3(e)] the E_1^+ splitting is as large as for the counter polarization, whereas for the as-grown sample [see Fig. 3(a)] the same emission line does not split at all! As a possible explanation for such an effect we suggest level coupling to *light-hole* states, as indicated in Fig. 8. It is known that the oscillator strength of light-hole optical transitions is about three times smaller than for heavy-holes.[47,48] Thus, light-hole transitions might not be resolved as a peak in PL spectra but they still have an indirect influence on the emission through the anti-crossing of heavy and light-hole states with the same component of the total angular momentum M_{L+j}, i.e., having the same symmetry. The fact that the behavior of the 700°C sample is in frankly contrast to that of the as-grown one clearly speaks for a change in shape or symmetry of the dots with annealing, such that the light-hole level moves away from the first excited heavy-hole state. Since, on the contrary, the overall splittings are essentially the same for all five samples, we infer that the annealing of the QD's leads mainly to an increase in dot height by Ga incorporation. For instance, this is also consistent with the observed saturation of the average exciton diameter with increasing annealing temperature, as determined from the diamagnetic shifts.

4. Conclusion

In summary, we have varied the Ga concentration and the shape of self-assembled InGaAs/GaAs QDs by annealing a given sample at different temperatures between 580 and 700°C. In this system, we have determined for the first time the magnetic-field shifts and splittings of the dot ground states and up to three excited levels. From our magnetoluminescence measurements at high excitation powers we conclude that the effect of annealing consists in the gradual incorporation of Ga into the dots while the dot shape changes mainly by growing in height. This is supported by the increase in the exciton diameter, the reduction of the effective g-factor of the ground state with annealing and the nearly constant magnetic splitting of excited-state PL lines. Although our magneto-PL data can be, in principle, described by a two-dimensional harmonic oscillator with envelope functions being characterized by the non vanishing z angular-momentum components, we obtained evidence from the ratio of the exciton diameters of the ground state and the first excited one that this model strictly applies only for the dot sample annealed at 700°C. Furthermore, the distinct magnetic-field behavior of the PL emission in σ^+ polarization from the recombination of the first excited state exciton at E_1 for the annealing series is indicative of a differently strong level coupling depending upon dot size and composition. In this way, from our magneto-PL experiments at high-power excitation on a series of annealed samples we have obtained further insight into the electronic properties of self-organized QDs. Results were analyzed using very simple models for the band structure and the magnetic-field interactions, which yielded important exciton parameters of the dots. For a deeper understanding, however, it would be necessary to take into account QD geometry as well as exciton-exciton interactions and many-body effects on the electrostatic confining potential, particularly in experiments at high-excitation power densities.

Acknowledgements

We thank O. Stier and A. L. Efros for helpful discussions. This work is supported by the Deutsche Forschungsgemeinschaft in the framwork of Sfb 296.

1) D. Bimberg, N. N. Ledentsov, M. Grundmann, N. Kirstaedter, O. G. Schmidt, M. H. Mao, V. M. Ustinov, A. Y. Egorov, A. E. Zhukov, P. S. Kopev, Z. I. Alferov, S. S. Ruvimov, U. Gösele and J. Heydenreich: Phys. Status Solidi B **194** (1996) 159.
2) D. Bimberg, M. Grundmann and N. N. Ledentsov: *Quantum Dot Heterostructures* (Wiley, New York, 1999).
3) D. J. Lockwood, P. Hawrylak, P. D. Wang, C. M. Sotomayor Torres, A. Pinczuk and B. S. Dennis: Phys. Rev. Lett. **77** (1996) 354.
4) S. Tarucha *et al.*: Physica E **3** (1998) 112.
5) U. Banin, Y.-W. Cao, D. Katz and O. Millo: Nature **400** (1999) 542.
6) U. Banin, C. J. Lee, A. A. Guzelian, A. V. Kadavanich, A. P. Alivisatos, W. Jaskolski, G. W. Bryant, A. L. Efros and M. Rosen: J. Chem. Phys. **109** (1998) 2306.
7) L.-W. Wang, J. Kim and A. Zunger: Phys. Rev. B **59** (1999) 5678.
8) O. Stier, M. Grundmann and D. Bimberg: Phys. Rev. B **59** (1999) 5688.
9) A. J. Williamson and A. Zunger: Phys. Rev. B **59** (1999) 15819.
10) V. Halonen, T. Chakraborty and P. Pietiläinen: Phys. Rev. B **45** (1992) 5980.
11) A. L. Efros, M. Rosen, M. Kuno, M. Nirmal, D. J. Norris and M. G. Bawendi: Phys. Rev. B **54** (1996) 4843.
12) M. Nirmal, D. J. Norris, M. Kuno, M. G. Bawendi, A. L. Efros and M.

Rosen: Phys. Rev. Lett. **75** (1995) 3728.
13) Y. Toda, S. Shinomori, K. Suzuki and Y. Arakawa: Appl. Phys. Lett. **73** (1998) 517.
14) Y. Toda, S. Shinomori, K. Suzuki and Y. Arakawa: Phys. Rev. B **58** (1998) R10147.
15) M. Bayer, A. Kuther, A. Forchel, A. Gorbunov, V. B. Timofeev, F. Schäfer, J. P. Reithmaier, T. L. Reinecke and S. N. Walck: Phys. Rev. Lett. **82** (1999) 1748.
16) S. Nomura, Y. Segawa and T. Kobayashi: Phys. Rev. B **49** (1994) 13571.
17) W. Heller and U. Bockelmann: Phys. Rev. B **55** (1997) R4871.
18) M. Bayer, A. Schmidt, A. Forchel, F. Faller, T. L. Reinecke, P. A. Knipp, A. A. Dremin and V. D. Kulakovskii: Phys. Rev. Lett. **74** (1995) 3439.
19) R. Rinaldi, P. V. Giugno, R. Cingolani, H. Lipsanen, M. Sopanen, J. Tulkki and J. Ahopelto: Phys. Rev. Lett. **77** (1996) 342.
20) A. Wojs, P. Hawrylak, S. Fafard and L. Jacak: Phys. Rev. B **54** (1996) 5604.
21) L. R. Wilson, D. J. Mowbray, M. S. Skolnick, M. Morifuji, M. J. Steer, I. A. Larkin and M. Hopkinson: Phys. Rev. B **57** (1998) R2073.
22) R. Rinaldi, R. Mangino, R. Cingolani, H. Lipsanen, M. Sopanen, J. Tulkki, M. Brasken and J. Ahopelto: Phys. Rev. B **57** (1998) 9763.
23) C. Ulrich, S. Ves, A. R. Goñi, A. Kurtenbach, K. Syassen and K. Eberl: Phys. Rev. B **52** (1995) 12212.
24) I. E. Itskevich, M. Henini, H. A. Carmona, L. Eaves, P. C. Main, D. K. Maude and J. C. Portal: Appl. Phys. Lett. **70** (1997) 505.
25) I. E. Itskevich, M. S. Skolnick, D. J. Mowbray, I. A. Trojan, S. G. Lyapin, L. R. Wilson, M. J. Steer, M. Hopkinson, L. Eaves and P. C. Main: Phys. Rev. B **60** (1999) R2185.
26) A. O. Kosogov, P. Werner, U. Gösele, N. N. Ledentsov, D. Bimberg, V. M. Ustinov, A. Y. Egorov, A. E. Zhukov, P. S. Kopev, N. A. Bert and Z. I. Alferov: Appl. Phys. Lett. **69** (1996) 3072.
27) R. Leon, D. R. M. Williams, J. Krueger, E. R. Weber and M. R. Melloch: Phys. Rev. B **56** (1997) R4336.
28) F. Heinrichsdorff, M. Grundmann, O. Stier, A. Krost and D. Bimberg: J. Cryst. Growth **195** (1998) 540.
29) S. J. Xu, X. C. Wang, S. J. Chua, C. H. Wang, W. J. Fan, J. Jiang and X. G. Xie: Appl. Phys. Lett. **72** (1998) 3335.
30) Z. Zhen *et al.*: Semiconductors **33** (1999) 80.
31) S. Fafard, Z. R. Wasilewski, C. N. Allen, D. Picard, M. Spanner, J. P. McCaffrey and P. G. Piva: Phys. Rev. B **59** (1999) 15368.
32) H. Born, A. R. Goñi, R. Heitz, A. Hoffmann, C. Thomsen, F. Heinrichsdorff and D. Bimberg: Phys. Status Solidi B **215** (1999).
33) O. Madelung: *Semiconductors — Basic Data* (Springer, Berlin, 1996).
34) A. R. Goñi and K. Syassen: Semicond. & Semimet. **54** (1998) 247.
35) A. R. Goñi, K. Strössner, K. Syassen and M. Cardona: Phys. Rev. B **36** (1987) 1581.
36) H. Eisele, O. Flebbe, T. Kalka, C. Preinesberger, F. Heinrichsdorff, A. Krost, D. Bimberg and M. Dähne-Prietsch: Appl. Phys. Lett. **75** (1999) 106.
37) H. Eisele, O. Flebbe, T. Kalka, F. Heinrichsdorff, A. Krost, D. Bimberg and M. Dähne-Prietsch: Phys. Status Solidi B **215** (1999) 865.
38) O. Madelung: *Introduction to Solid-State Theory* (Springer, Berlin, 1978).
39) A. R. Goñi, K. Syassen, Y. Zhang, K. Ploog, A. Cantarero and A. Cros: Phys. Rev. B **45** (1992) 6809.
40) T. Wimbauer, K. Oettinger, A. L. Efros, B. K. Meyer and H. Brugger: Phys. Rev. B **50** (1994) 8889.
41) D. M. Hofmann, K. Oettinger, A. L. Efros and B. K. Meyer: Phys. Rev. B **55** (1997) 9924.
42) K. W. Böer: *Survey of Semiconductor Physics* (Van Nostrand Reinhold, New York, 1990) Vol. I.
43) M. Willatzen, M. Cardona and N. E. Christensen: Phys. Rev. B **50** (1994) 18054.
44) M. Willatzen, M. Cardona and N. E. Christensen: Phys. Rev. B **51** (1995) 17992.
45) A. A. Sirenko, T. Ruf, N. N. Ledentsov, A. Y. Egorov, P. S. Kopev, V. M. Ustinov and A. E. Zhukov: Solid State Commun. **97** (1996) 169.
46) R. Heitz and H. Born: private communication.
47) O. J. Glembocki and B. V. Shanabrook: Semicond. & Semimet. **36** (1992) 221.
48) C. Ulrich, A. R. Goñi, K. Eberl and K. Syassen: *High Pressure Science and Technology*, ed. W. A. Trzeciakowski (World Scientific, Singapore, 1996) p. 647.